Calculation of crystal field splittings in distorted coordination polyhedra: spectra and thermodynamic properties of minerals

BERNARD J. WOOD

Department of Geology, The University, Manchester M13 9PL, England

AND R. G. J. STRENS

School of Physics, The University, Newcastle NE1 7RU, England

SUMMARY. A simple method has been developed for calculating the d-orbital energy levels of transition-metal ions in coordination polyhedra with both orthogonal and non-orthogonal distortions, using equations based on those derived by Ballhausen (1954). The input data are atomic coordinates, a standard value of the crystal field splitting parameter Δ at known metal–ligand distance, and the ratio of radial integrals B_2/B_4, which is approximately constant for a given ion. The method can be applied to polyhedra containing different ligands.

Application of the equations to the Mn^{3+} ($M3$) site in piemontite and the Fe^{2+} ($M2$) site in ortho-pyroxene gives calculated transition energies in good agreement with the observed band energies.

The calculations permit definite assignment of the great majority of d–d absorption bands even in multi-site phases, and enable discrimination of crystal-field and charge-transfer bands in mineral spectra. They also throw light on the fine structures of both oxygen → metal and metal → metal charge-transfer bands, and allow the calculation of crystal-field stabilization enthalpy and electronic entropy. The latter is a previously neglected energy term that contributes significantly to the energetics of reactions within and between phases containing transition-metal ions.

THE dominant features of the spectra of silicate minerals in the near ultra-violet, visible, and near infrared are determined mainly by the presence of first-row transition-metal ions, the most abundant species being Fe^{2+} and Fe^{3+}. These ions contribute three main features to the spectra.

First, the oxygen → metal charge-transfer process gives very strong absorption bands in the near-ultra-violet, the low-energy tails of which are responsible for the background absorption in the visible and infrared. These bands occur near 5·5 eV (Fe^{3+}) and 7·0 eV (Fe^{2+}), and have oscillator strengths $f \approx$ 0·1 to 0·3.

Second, the metal → metal charge-transfer absorption appears as sharp bands, usually in the visible, superimposed on the background due to the O → M absorption. These arise from the photon-assisted transfer of electrons between metal ions in

adjacent coordination polyhedra, e.g. $Fe^{2+} \rightarrow Fe^{3+}$ (Robbins and Strens, 1968, 1972; Faye *et al.*, 1968), and $Fe^{2+} \rightarrow Ti^{4+}$ in kyanite (G. Smith, Newcastle University, unpublished). These bands have oscillator strengths of $f \approx 0.001$, with band widths of 3000 to 5000 cm^{-1} in most cases.

Finally, there are bands attributed to transitions between the *d*-orbital energy levels of transition-metal ions occupying the (usually) distorted coordination polyhedra in minerals. These again appear as relatively narrow (width 400 to 2000 cm^{-1}) bands superimposed on the background of $O \rightarrow M$ absorption. Oscillator strengths range from $f \approx 0.001$ for spin- and symmetry-allowed bands, to $f \approx 10^{-7}$ for spin-forbidden, symmetry-forbidden bands. Most of the available spectral data for *d–d* bands have been summarized by Burns (1970).

Although the present work deals only with the calculation of *d*-orbital energy levels, it has applications to all the types of spectra mentioned above since the fine structure of the $O \rightarrow M$ and $M \rightarrow M$ charge-transfer spectra is largely determined by the *d*-orbital splittings of the acceptor ions. The method of calculation is a further development of methods outlined by Strens (1968) and Strens and Wood (1969). Applications to ferromagnesian silicates and to minerals containing ions other than Fe^{2+} will be dealt with elsewhere (Wood and Strens, in preparation; Wood, 1971, and in press).

Outline of the problem

The relative energies of the five *d*-orbitals in regular octahedral, tetrahedral, and cubic eightfold coordination are shown in fig. 1. The electrostatic repulsion between the *d*-electrons and the negatively charged ligands causes an increase of nze/R in the energy of the *d*-orbitals, where n is the number of ligands, z their charge, and R is the metal–ligand distance. In all three types of site, the *d*-orbitals are split into two groups, t_{2g} or d_ϵ and e_g or d_γ. Relative to the baricentre, the t_{2g} orbitals are stabilized by $2\Delta/5$, and the e_g orbitals are destabilized by $3\Delta/5$ in octahedral sites. The stabilizations have the opposite sign in tetrahedral and cubic sites.

As a site is distorted from regular symmetry, further splitting of the *d*-orbitals occurs, until in orthorhombic, monoclinic, or triclinic point-groups all five energy levels are non-degenerate. Each distorted site in a multi-site phase can then contribute up to four spin-allowed *d–d* transitions in the case of d^4 or d^6 ions, e.g. Mn^{3+} and Fe^{2+}. The observed spectra of silicates containing transition-metal ions may therefore become very complex, and *d–d* absorption bands cannot be assigned unequivocally by the purely empirical methods in common use. Indeed, some authors have been unable to distinguish between *d–d* and charge-transfer bands.

An example of such differences in assignment is provided by the band at about 5000 cm^{-1} in pyroxenes, which was originally attributed by White and Keester (1966) to the $^5E \rightarrow {}^5T_2$ transition of tetrahedrally coordinated Fe^{2+}, and later reassigned by Bancroft and Burns (1967) to a transition between the non-degenerate '*t*' levels of Fe^{2+} in the distorted octahedral $M2$ site. Our calculations confirm the latter assignment, but differ in detail (notably the assignment of electronic axes) from the earlier work.

A second area of confusion lies in the discrimination of d–d and charge-transfer bands, particularly in the spectra of tourmaline, cordierite, kyanite, and corundum. Our calculations, taken with recent work by G. Smith, enable definite assignments to be made for these minerals.
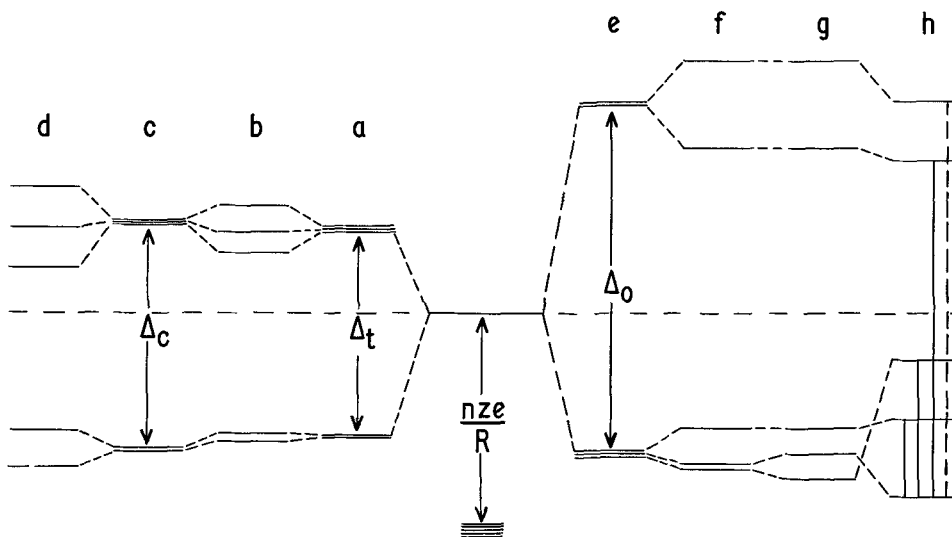

FIG. 1. Calculated d-orbital energy levels relative to the baricentre in a selection of regular and distorted coordination polyhedra: regular tetrahedron (a); distorted tetrahedron in staurolite (b); eightfold cubic coordination (c); eightfold site in pyrope (d); regular octahedron (e); tetragonally distorted octahedron with $R_x = R_y = 0.97 R_z$, and $\Delta_x = \Delta_y = 10\,500$ cm^{-1} and $\Delta_z = 9000$ cm^{-1} (f); orthorhombically distorted octahedron with $R_x : R_y : R_z = 0.98 : 1 : 1.02$, and $\Delta_x \approx 11\,000$, $\Delta_y = 10\,000$ and $\Delta_z \approx 9000$ cm^{-1} (g); and (h) the octahedron about the $M(2)$ position in orthopyroxene, showing also the allowed and forbidden (dashed) optical transitions of Fe^{2+} in this site.

Method of calculation

Ballhausen (1954) used a point-charge approximation to calculate d-orbital energy levels for fields of different symmetry, and applied his findings to the interpretation of the spectra of cupric compounds, in which Cu^{2+} normally occupies strongly distorted octahedra. On rearranging Ballhausen's equations an expression of the form

$$Energy = n_x(B_0 + C_1 B_2 + C_2 B_4) + n_y \ldots$$

is obtained, containing three independent energy terms, one for each of the three Cartesian axes (x, y, z) of the point group. Here, n_x is the number of ligands on the x axis (not necessarily an integer), B_0, B_2 and B_4 are the appropriate radial integrals, and C_1, C_2 are constants. The energies of all five d-orbitals as a function of these parameters are given in Table I. In a regular octahedron, $n_x = n_y = n_z = 2$, and the expressions of Table I reduce to the familiar result of one doublet state and one triplet with energies $E_g = 6B_0 + B_4$, $T_{2g} = 6B_0 - 2B_4/3$. The B_0 terms simply give the increase in energy of the set as a whole due to the spherical potential of the ligands,

and they can therefore be dropped from arguments concerned only with the d–d splittings. Hence, $\Delta = 5B_4/3$ or $B_4 = 0\cdot6\Delta$. The magnitude of B_2 is not so easily determined, but Ballhausen's expressions for the radial integrals give the ratio $B_2/B_4 = 2x^2/75$. Here $x = ZR/3$, where R is the metal–ligand distance in atomic units,

TABLE I. *Energies of d orbitals in terms of radial integrals;*
adapted from Ballhausen (1954)

$n_{x,y,z} =$ no. of ligands on x, y, z axes

z^2 $n_x(B_0 - \frac{1}{7}B_2 + \frac{3}{28}B_4) + n_y(B_0 - \frac{1}{7}B_2 + \frac{3}{28}B_4) + n_z(B_0 + \frac{2}{7}B_2 + \frac{2}{7}B_4)$

$x^2 - y^2$ $n_x(B_0 + \frac{1}{7}B_2 + \frac{19}{84}B_4) + n_y(B_0 + \frac{1}{7}B_2 + \frac{19}{84}B_4) + n_z(B_0 - \frac{2}{7}B_2 + \frac{1}{21}B_4)$

xy $n_x(B_0 + \frac{1}{7}B_2 - \frac{4}{21}B_4) + n_y(B_0 + \frac{1}{7}B_2 - \frac{4}{21}B_4) + n_z(B_0 - \frac{2}{7}B_2 + \frac{1}{21}B_4)$

xz $n_x(B_0 + \frac{1}{7}B_2 - \frac{4}{21}B_4) + n_y(B_0 - \frac{2}{7}B_2 + \frac{1}{21}B_4) + n_z(B_0 + \frac{1}{7}B_2 - \frac{4}{21}B_4)$

yz $n_x(B_0 - \frac{2}{7}B_2 + \frac{1}{21}B_4) + n_y(B_0 + \frac{1}{7}B_2 - \frac{4}{21}B_4) + n_z(B_0 + \frac{1}{7}B_2 - \frac{4}{21}B_4)$

Expressions for d-orbital energies in an orthogonally distorted octahedron when
$B_2/B_4 = 2$. *Note that* $n_x = n_y = n_z = 2$. *For tetrahedral and cubic eightfold sites*
multiply all energies by minus two-thirds

$$z^2 = -0\cdot214\Delta x \quad -0\cdot214\Delta y \quad +1\cdot028\Delta z$$
$$x^2 - y^2 = +0\cdot614\Delta x \quad +0\cdot614\Delta y \quad -0\cdot628\Delta z$$
$$xy = +0\cdot114\Delta x \quad +0\cdot114\Delta y \quad -0\cdot628\Delta z$$
$$xz = +0\cdot114\Delta x \quad -0\cdot628\Delta y \quad +0\cdot114\Delta z$$
$$yz = -0\cdot628\Delta x \quad +0\cdot114\Delta y \quad +0\cdot114\Delta z$$

and Z is the effective nuclear charge on the cation, which may be calculated approximately by Slater's (1930) method. However, the B_2/B_4 ratio is best regarded as an empirical parameter to be fitted to the spectrum (Basolo and Pearson, 1967). Calculated values of this ratio for some of the more important ions range from 1·6 to 2·7, with Fe^{2+} occupying an intermediate position at 2·0. Knowing B_4 and the B_2/B_4 ratio, the expression for the energy becomes

$$E = \tfrac{3}{5}\Delta_x[C_1 B_2/B_4 + C_2] + \tfrac{3}{5}\Delta y \ldots,$$

where $n_x\Delta_0$ has been replaced by Δ_x. The energy levels of ions in orthogonally distorted sites can now be calculated, provided the dependence of Δ on metal–ligand distance is known. If the surrounding ligands are approximated to point charges, Δ varies as R^{-5}, whilst a point dipole approximation yields $\Delta \propto R^{-6}$. Drickamer (1965) has determined the change in Δ with R for transition metal ions in oxides, and has shown that the R^{-5} dependence holds over the experimentally accessible ranges of R, and we have therefore assumed inverse fifth-power dependence of Δ on R.

On this assumption, and taking $B_2/B_4 = 2\cdot0$, the effect of a tetragonal distortion of an octahedron on the d-orbital energy levels is shown in fig. 2. Movement of the ligands on the z-axis away from the central ion leaves n_z unchanged, but reduces Δ_z as $(R_0/R_z)^5$, stabilizing d_{z^2} relative to $d_{x^2-y^2}$, and $d_{xz,yz}$ relative to d_{xy}. Compression along the z-axis (e.g. Mn^{3+} in piemontite) has the opposite effect, stabilizing $d_{x^2-y^2}$ and d_{xy}.

A purely orthogonal distortion model is a reasonable approximation for a number of octahedral sites in silicates, e.g. olivine $M(1)$, hypersthene $M(1)$, and piemontite $M(3)$, but there are many in which large non-orthogonal components are present. The key to the solution of this problem lies in the calculation of n_x, n_y and n_z, since these obviously vary as ions are moved off the orthogonal axes. Since $n_x + n_y + n_z$ must remain constant and equal to the coordination number, and (at constant R) the interaction energy nze/R must also be conserved, we find that the contributions of the ions to Δ_x must be weighted according to $\cos^2\theta_i$, where θ_i is the angle between the ith metal–ligand vector, and the x-axis. The full expression for Δ_x then becomes:

$$\Delta_x = \sum_i \Delta_0 (R_0/R_i)^5 \cos^2\theta_i.$$

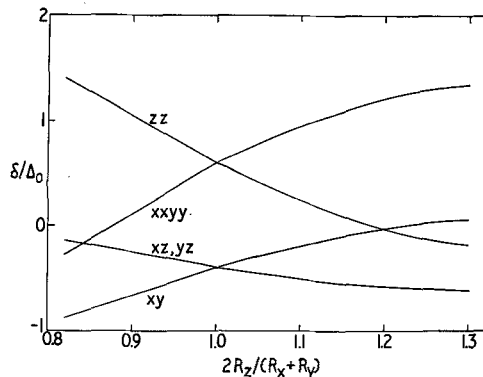It is therefore necessary to assume some standard value of Δ_0 at a known R for

FIG. 2. Calculated d-orbital energy levels relative to the baricentre (in units of Δ_0) in tetragonally distorted octahedra, as a function of $2R_z/(R_x + R_y)$, with $B_2/B_4 = 2$. Here, $z^2 = zz$, and $x^2 - y^2 = xxyy$.

the ion under consideration. In particular, the use of $\Delta_0 = 9750$ cm^{-1} at $R_0 = 2 \cdot 135$ Å, with $B_2/B_4 = 2 \cdot 0$ has enabled accurate calculations to be made of the energies of the great majority of absorption bands in Fe^{2+} silicates.

TABLE II. *Calculated d-orbital energy levels in piemontite M(3) and hypersthene M(2) sites in cm^{-1} relative to baricentre*

| Piemontite $M(3)$		Hypersthene $M(2)$	
z^2	14075	x^2-y^2 (B_1)	6121
x^2-y^2	2001	z^2 (A_1)	4405
yz	-3420	yz (A_2)	-1301
xz	-4175	xy (A_1)	-2997
xy	-8475	xz (B_2)	-6231
Δ_0	12800 cm^{-1}	Δ_0	9750 cm^{-1}
R_0	2·06 Å	R_0	2·135 Å
B_2/B_4	1·60	B_2/B_4	2.00
z	O(8)–$M(3)$–O(4)	z	[010]
y	[010]	y	$M(2)$–O(5)
Symmetry	C_s	Symmetry	C_1

Atomic coordinates were taken from Ghose (1965) and Dollase (1969).

Applications

As illustrations of the method it is appropriate to take one site with a strong tetragonal distortion, and one with a more complex non-orthogonal distortion.

The Mn^{3+} ($M3$) site in *piemontite* is shown in fig. 3, with bond lengths according to Dollase (1969). The site has formal symmetry C_s, with the mirror plane normal to b, but the principal distortion is the strong tetragonal compression along the o(8)–$M(3)$–O(4) axis. The unique direction normal to the plane of symmetry would normally be assigned as the electronic z axis, but it was found necessary to place z along the pseudo-tetrad axis of compression, with $y = b$ in order to obtain agreement between calculated and observed energies.
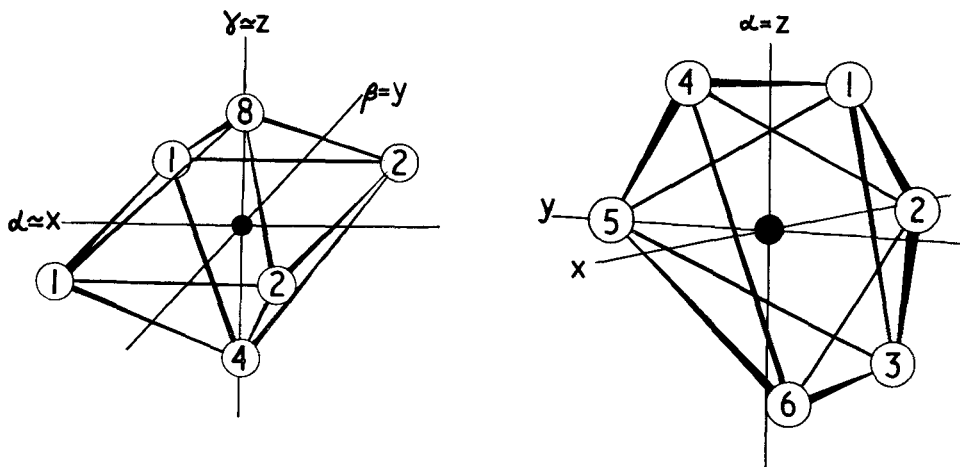
FIGS. 3 and 4: FIG. 3 (left). The octahedron about the $M(3)$ position in piemontite, showing the orientation of electronic axes used in the calculation. Dollase (1969) found the following metal (M) to oxygen distances in a piemontite with *ca*. ($Mn_{0.76}Fe_{0.07}Al_{0.17}$) in the $M(3)$ site: $2 \times M$–O(1) = 2·274, $2 \times M$–O(2) = 2·031, M–O(4) = 1·900, M–O(8) = 1·861 Å. FIG. 4 (right). The octahedron about the $M(2)$ position in hypersthene, showing the orientation of electronic axes used in the calculation. Ghose (1965) found M–O(1) = 2·14, M–O(2) = 2·07, M–O(3) = 2·52, M–O(4) = 2·18, M–O(5) = 2·04, and M–O(6) = 2·41 Å.

The calculated B_2/B_4 ratio is 1·62, and a value of 1·6 was found to give an excellent fit to the spectrum with $\Delta_0 = 12\ 800\ cm^{-1}$ at $R_0 = 2·06$ Å. The calculated and observed band positions are compared in Table III, using the spectral data of Burns and Strens (1967).

In C_s symmetry the 12 000 cm^{-1} transition is allowed only in $y(\beta)$ polarization, which is the observed orientation of maximum intensity. Band 2 should be present in all spectra, with band 1 α and γ polarized. Band 1 is in fact α and β polarized, implying some relaxation of the selection rules, possibly involving the mechanism of substitutional intensification discussed by Robbins and Strens (1972). Site symmetries other than C_s were tried, but failed to give better agreement between observed and predicted polarizations.

The spectrum of Fe^{2+} in *bronzite* was determined by Bancroft and Burns (1967), and has two main bands near 5000 and 11 000 cm^{-1}. A third band at 3100 cm^{-1} was located by White and Keester (1966), but its polarization was not determined. Since iron is strongly concentrated in the $M(2)$ position of orthopyroxene, and the $M(1)$

position is centrosymmetric (and so expected to contribute only weak vibronic bands to the spectrum), these bands are assigned to Fe^{2+} in $M(2)$. The highly distorted $M(2)$ site is shown in fig. 4, using distances from Ghose (1965). The formal symmetry is C_1, but there is C_{2v} pseudo-symmetry with a diad along $b = \alpha$. This direction was therefore taken as electronic z, with y along the short metal–oxygen distance $M(2)$–$O(5)$. The calculated energy levels on the basis of these assignments are given in Table II. The B_2/B_4 ratio was set at 2·0 (1·98 calculated), with $\Delta_0 = 9750$ cm^{-1} at $R_0 = 2\cdot135$ Å.

TABLE III. *Comparison of observed and calculated band parameters*

Piemontite:

Band	Observed				Calculated		
	α	β	γ	polarization	ν_{calc}	assignment	polarization
1	22 000	22 200	—	$\beta > \alpha$	22550	$z^2 \leftarrow xy$	α, γ
2	18 700	17 800	18 250	$\gamma \simeq \beta > \alpha$	$\begin{cases} 18\,250 \\ 17\,495 \end{cases}$	$\begin{matrix} z^2 \leftarrow xz \\ z^2 \leftarrow yz \end{matrix}$	α, β, γ
3	12 580	11 900	—	$\beta \gg \alpha$	12 074	$z^2 \leftarrow x^2 - y^2$	β

Optic orientation: $\beta = b$, $\alpha \wedge c = 5°$, $\gamma \wedge a = 30°$.

Hypersthene:

Band	Observed				Calculated		
	α	β	γ	polarization	ν_{calc}	assignment	polarization
	—	—	—	—	12 352	$xz \rightarrow x^2 - y^2$	forbidden
1	10 790	11 150	11 200	$\alpha > \beta > \gamma$	10 636	$xz \rightarrow z^2$	α
2	—	5380	5300	$\beta > \gamma \gg \alpha$	4930	$xz \rightarrow yz$	$\frac{3}{4}\beta, \frac{1}{4}\gamma$
3	(3100)	—	—	undetermined	3234	$xz \rightarrow xy$	α

Optic orientation: $\alpha = b$, $\beta = a$, $\gamma = c$.

The selection rules and polarization dependence of transitions have been discussed by White and Keester (1967), but our interpretation differs from theirs in the assignment of axes. Using the descent of symmetry tables (Wilson, Decius, and Cross, 1955) the five d-orbitals transform as the following states:

$$z^2 = A_1; \quad x^2 - y^2 = B_1; \quad xy = A_1; \quad yz = A_2; \quad xz = B_2.$$

The ground state is thus B_2, and the B_2 to A_1 (11 000 cm^{-1}) transition is allowed along $B_2 = z = b = \alpha$, which is the observed direction of maximum intensity. The B_2 to A_2 (4900 cm^{-1}) transition is allowed along $x \approx \frac{3}{4}a + \frac{1}{4}c$, with the B_2 to A_1 (3100 cm^{-1}) transition polarized along $z = \alpha$. The latter has not yet been observed in polarized light, but the former has high intensity along $a = \beta$ and moderate intensity along $c = \gamma$, in agreement with prediction. The high energy (B_2 to B_1) transition (not observed) is forbidden in all three polarizations in C_{2v} symmetry.

Thermodynamic properties

The quality usually called the 'crystal field stabilization energy' is in fact an enthalpy, denoted here by H_{cf}. In the general case $H_{cf} = \sum_i \epsilon_i n_i$, where ϵ_i is the energy of the ith orbital relative to the baricentre, and n_i is the number of electrons in that orbital. For high-spin Fe^{2+} at low temperature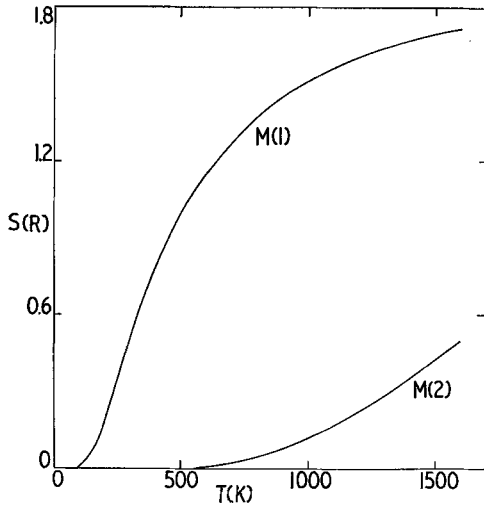s, the 'sixth' electron is localized in the ground state, with energy ϵ_0, and $H_{cf} = \epsilon_0$, since the contribution of the first five electrons sums to zero. Both ϵ_i and n_i are functions of temperature, and H_{cf} therefore varies with temperature.

At temperatures such that kT is comparable with the splittings of the lowest-lying orbitals, the electron distribution becomes partially disordered, contributing an electronic entropy:

$$S_{el} = -R \sum_i n_i \ln n_i + (1-n_i)\ln(1-n_i).$$

For high-spin Fe^{2+} compounds, only the 'sixth' d-electron need be considered and the maximum entropy contribution at geologically reasonable temperatures is 2·8 to 3·8 e.u. At 1000 °K, the $T(S_1-S_2)$ term can contribute as much as 3 kcal/mole to exchange energies between a distorted site with large d-orbital splittings, and an undistorted site with small splittings (fig. 5).

FIG. 5. The calculated electronic entropy, in units of the gas constant R, attributable to Fe^{2+} in the $M(1)$ and $M(2)$ sites of hypersthene.

Discussion and conclusions

The strong distortions of the piemontite $M(3)$ and orthopyroxene $M(2)$ sites provide a severe test of the method of calculating d-orbital energy levels, and the agreement between observed and calculated values is most satisfactory. Even the discrepancies that remain are attributable in part to differences between the average ligand–metal distances as determined by X-ray methods and the distances in those sites that are occupied by Mn^{3+} and Fe^{2+} ions. Indeed, the comparison of observed and calculated band energies can be used to investigate the relaxation of mineral structures around transition metal ions replacing Mg^{2+} in cordierite and Al^{3+} in epidotes (Wood, 1971).

Differences of several hundred wavenumbers occur between calculated and observed band energies for a number of minerals containing Fe^{2+} in centrosymmetric sites, due to the effects of vibronic coupling: $\nu_{obs} = \nu_{el}+\nu_{vib}$. The effect is particularly important in pyrope, and our calculated H_{cf} for this mineral is likely to be more accurate than values derived from the spectra.

Experience gained in applying the calculations to a wide range of ions and coordination numbers (Wood, 1971, 1972) suggests that the point-charge model holds

well so long as the formal charge per bond (i.e. ionic charge/coordination number) does not greatly exceed one-half. The only case in which the point-charge calculations failed was that of the spinel Fe_2GeO_4, a highly symmetrical structure in which polarization effects are important. No evidence was found for significant polarization (or next-nearest neighbour) effects in any silicate structure. Neither was there any indication that the state of chemical combination of the oxygen ions in these structures mattered, for the same values of Δ_0 and R_0 were used for oxygen ions in hydroxyl groups and water molecules, and for both bridging and non-bridging ions in the complex silicate anions present in pyroxenes and amphiboles.

The application of the calculations to phase-equilibrium and thermodynamic properties of minerals has been discussed by Strens (1969), Wood (1971), and Wood and Strens (1969, 1971).

REFERENCES

BALLHAUSEN (C. J), 1954. *Kgl. Danske Viderskab. Selskab. Mat. Fys. Medd.* **29,** 3–18.
BANCROFT (G. M.) and BURNS (R. G.), 1967. *Amer. Min.* **52,** 1278–87.
BASOLO (F.) and PEARSON (R. G.), 1967. *Mechanisms of inorganic reactions*, 2nd edn, New York (Wiley).
BURNS (R. G.), 1970. *Mineralogical applications of crystal field theory*. London (Cambridge University Press).
—— and STRENS (R. G. J.), 1967. *Min. Mag.* **36,** 204–26.
DRICKAMER (H. G.), 1965. *Solid State Phys.* **17,** 1–133.
DOLLASE (W. A.), 1969. *Amer. Min.* **54,** 710–17.
DUNITZ (J. D.) and ORGEL (L. E.), 1957. *Journ. Phys. Chem. Solids*, **3,** 318–33.
FAYE (G. H.), MANNING (P. G.), and NICKEL (E. H.), 1968. *Amer. Min.* **53,** 1174–1201.
GHOSE (S.), 1965. *Zeits. Krist.* **122,** 81–89.
ROBBINS (D. W.) and STRENS (R. G.), 1968. *Chem. Commun.* 508–9.
—— —— 1972. *Min. Mag.* **38,** 551–63.
SLATER (J. D.), 1930. *Phys. Rev.* **36,** 57–64.
STRENS (R. G. J.), 1968. Abstracts, 6th general meeting I.M.A., 127.
—— 1969. In *Application of modern physics to the Earth and planetary interiors*. S. K. RUNCORN (ed.), London (Wiley).
—— and WOOD (B. J.), 1969. Abstract, amphibole and pyroxene symposium, Blacksburg. *Amer. Min.* **55,** 313–14.
WHITE (W. B.) and KEESTER (K. L.), 1966. Ibid. **51,** 555–58.
—— —— 1967. Ibid. **52,** 1508–14.
WILSON (E. B.), DECIUS (J. C.), and CROSS (P. C.), 1955. *Molecular vibrations*, New York (McGraw Hill).
WOOD (B. J.), 1971. Ph.D. thesis, University of Newcastle upon Tyne.
—— 1973. In press.
—— and STRENS (R. G. J.), 1969. Abstract, amphibole and pyroxene symposium, Blacksburg. *Amer. Min.* **55,** 316.
—— —— 1971. *Earth Planet. Sci. Letters*, **11,** 1–6.